

Annealing of GaN under high pressure of nitrogen

This article has been downloaded from IOPscience. Please scroll down to see the full text article.

2002 J. Phys.: Condens. Matter 14 11097

(<http://iopscience.iop.org/0953-8984/14/44/433>)

View [the table of contents for this issue](#), or go to the [journal homepage](#) for more

Download details:

IP Address: 171.66.16.97

The article was downloaded on 18/05/2010 at 17:15

Please note that [terms and conditions apply](#).

Annealing of GaN under high pressure of nitrogen

S Porowski, I Grzegory, D Kolesnikov, W Lojkowski, V Jager, W Jager,
V Bogdanov, T Suski and S Krukowski

High Pressure Research Center, Polish Academy of Sciences, Sokolowska 29/37,
01-142 Warsaw, Poland

Received 11 June 2002

Published 25 October 2002

Online at stacks.iop.org/JPhysCM/14/11097

Abstract

Gallium nitride, aluminum nitride and indium nitride are basic materials for blue optoelectronic devices. The essential part of the technology of these devices is annealing at high temperatures. Thermodynamic properties of the Ga–N system and their consequences to application of high nitrogen pressure for the annealing of GaN based materials are summarized.

The diffusion of Zn, Mg and Au in high dislocation density heteroepitaxial GaN/Al₂O₃ layers will be compared with the diffusion in dislocation-free GaN single crystals and homoepitaxial layers. It will be shown that high dislocation density can drastically change the diffusion rates, which strongly affects the performance of nitride devices.

Inter-diffusion of Al, Ga and In in AlGaN/GaN and InGaN/GaN quantum well (QW) structures will be also considered. It will be shown that in contrast to stability of metal contacts, which is strongly influenced by dislocations, the inter-diffusion of group III atoms in QW structures is not affected strongly by the presence of high dislocation density. This is related to the different rate controlling slow process in these two diffusion processes. This feature of interdiffusion processes explains the success of heteroepitaxial techniques in the technology of nitride based light emitting diodes.

1. Introduction

Gallium nitride and its solid solutions with AlN and InN constitute the material basis of optoelectronic device technology developed in the last ten years. Starting from discovery of activation of p-type doping by electron irradiation [1] and hydrogen-free annealing [2], the technological development led to the construction of blue, green and amber light emitting diodes (LEDs) [3, 4]. These diodes are accessible commercially at present. Also low power blue laser diodes (LDs) were constructed [5]. The latter devices are not yet developed to the technological stage, allowing for mass production and commercial distribution.

Due to inaccessibility of substrate quality GaN single crystals in large quantities fast progress in LED nitride technology is based on heteroepitaxial metal–organic chemical vapour

deposition (MOCVD) growth techniques using Al_2O_3 (sapphire) or SiC substrates. Lattice mismatch between the substrate and the nitride layer is large, equal to 14% in the case of sapphire and 3.4% in the case of SiC. Therefore special procedures were developed, including deposition of a low temperature buffer layer, and subsequent recrystallization during annealing. Then the proper device structure was deposited, where the dislocation density was of the order of 10^9 – 10^{10} cm^{-2} . Despite very high dislocation density, GaN/InGaN/GaN single-quantum-well (QW) based devices have high quantum efficiency. The possible explanation of this effects is still disputed [6].

LDs are based on multiquantum well (MQW) InGaN structures, and therefore impose much more stringent criteria on the structural quality of the active layers. Additionally the optical waveguides have to be grown. This is accomplished using AlGaIn layers. Therefore, the defect densities which are acceptable for LEDs are not acceptable for LDs. In consequence, sophisticated growth methods were developed, including epitaxial layer overgrowth (ELOG), which allows us to decrease dislocation density in the active layers to about 10^5 – 10^6 cm^{-2} [7]. These dislocation densities are still high and make fabrication of high power blue laser and UV LEDs very difficult.

The possible solution is to use GaN substrates. Growth of GaN single crystals is very difficult, due to thermodynamic properties of the Ga–N system. N_2 is the strongest bonded diatomic molecule and this favours the decomposition of GaN into Ga and N_2 . In order to prevent GaN decomposition, high nitrogen pressures are necessary, especially when high temperatures are used. Low temperature growth is possible using sources of active nitrogen, such as ammonia. Unfortunately, low temperature methods were not successful in growth of substrate quality GaN single crystals. The alternative is to use high temperature and high nitrogen pressure to synthesize GaN from its constituents. At present this is the only method by which ~ 10 mm size GaN substrate quality crystals have been obtained. This method is discussed in a parallel publication [8]. Since the availability of pressure grown substrates is still limited, homoepitaxial growth has been used in a relatively limited number of attempts [9]. Therefore, the impact of this development on the investigation of the properties of the nitride layer is still limited.

Magnesium is the acceptor impurity used in virtually all present day p-type GaN layers [1, 2]. Doping with Mg in MOCVD processes, in the presence of NH_3 , leads to creation of Mg–H complexes, in which H behaves as a donor [10]. This lowers the energy of the complex, allowing introduction of more Mg during growth of the layers. Afterwards, Mg can be activated by annealing in hydrogen free atmosphere, using temperatures close to 800°C [11]. Other possible p-type impurities include Zn and Be [12, 13]. However, all attempts to obtain useful p-type nitrides with these impurities have not been successful. For n-type doping, Si is commonly used [14]. These impurities are introduced during growth of the active layers of the optoelectronic devices. The p–n diode structure, which is the base of all optoelectronic devices, requires that the impurity profile remains sharp during all processing procedures of the devices. Therefore understanding of the diffusion of both p-type and n-type impurities has to be controlled.

Similarly to the p–n junctions, the MQW structures, consisting of AlGaIn and InGaIn layers, should remain unaffected during annealing procedures, necessary for fabrication of LDs. Since, for good performance of the devices, the interfaces between these layers have to be atomically flat, the nondiffusion requirements are particularly stringent in this case. Therefore determination of the conditions allowing the inter-diffusion of group III metal atoms is very important.

The technology of the nitride based optoelectronic devices includes also doping by ion implantation. Doping by implantation is used for the preparation of the conductive nitride

layer in the vicinity of the metal contacts. Doping by implantation entails the introduction of foreign atoms and damage to the implanted layers. The damage has to be removed and the impurity atoms have to find their way to proper lattice positions. In contrast to the previous cases, this requires a certain level of mobility of all atoms in the lattice. As has been shown before [15], the effective removal of the implantation damage requires use of a temperature close to 1300 °C. Although the annealing time is short (of the order of 10 s), this process sets the upper limit for the temperature–time annealing process, which can be used as a benchmark for the stability of the nitride structures.

A final element of the nitride technology relevant to the diffusion processes discussed here is the formation of the contacts to p-type and n-type GaN layers. For p-type nitrides the Ni/Au whereas for n-type Ti/Au or Al/Au contacts can be used. Therefore the diffusion of these metals into the heavily dislocated or dislocation free layers is important. The results presented in this paper prove that the diffusion of the metal depends crucially on the presence of dislocations in the nitride layers.

2. Thermodynamic properties of Ga–N system and annealing procedures

Gallium nitride, indium and aluminum nitride have similar properties. This is in part related to the properties of nitrogen. The nitrogen molecule is the strongest bonded diatomic molecule—the N_2 dissociation energy is equal to 9.8 eV. This affects the thermodynamic properties of the Ga–N system. The high binding energy of N_2 favours the existence of gaseous nitrogen, therefore the nitrogen pressures required for GaN stability are high, especially at higher temperatures. According to the standard thermodynamic formulae the product of $p_{Ga} p_{N_2}^{1/2}$, sufficient for GaN stability, is uniquely determined by the temperature of the crystal. Therefore the partial pressure of nitrogen depends on the partial pressure of gallium. The lowest possible nitrogen pressure corresponds to triple-phase equilibrium $GaN(s)–N_2(g) \cdot Ga(g)–Ga:N(l)$, where g denotes gas phase, s solid GaN and the third phase (l) is nitrogen solution in liquid Ga. Since, as we shall see later, the technically accessible annealing temperatures are much lower than the GaN melting temperature, the nitrogen solution is very dilute. Therefore the pressure of Ga over pure Ga(l) can be used as a good approximation of the partial pressure of Ga in the triple-point equilibrium.

The equilibrium pressure of Ga over GaN is relatively low, showing that the vapourization of Ga is an energy costly and slow process. This is very fortunate from the point of view of annealing experiments, because Ga evaporation during GaN sublimation, being very slow, can be easily prevented in most experiments. The partial pressure of Ga derived from standard thermodynamic tables is shown in figure 1 [21]. As shown the Ga pressure follows the van t'Hoff relation, according to which the logarithm of the equilibrium pressure is a linear function of the inverse of the temperature.

Because the saturation pressure over liquid Ga can be determined as a function of temperature, the lowest equilibrium N_2 pressures over GaN can be also expressed uniquely as a function of the temperature. The corresponding N_2 pressure, determined experimentally by Karpinski *et al* [22], is also presented in figure 1. One can note that the nitrogen pressures are many orders of magnitude higher than the gallium pressures. For low N_2 pressures the van t'Hoff relation is obeyed but for higher pressures the properties of N_2 gas deviate strongly from the ideal gas behaviour. This is beneficial from the point of view of GaN stability, because N_2 pressure are one order of magnitude lower than those resulting from the van t'Hoff ideal gas relation, estimated for a typical experimental temperature range, close to 1800 K.

One has to note that gallium nitride is a strongly bonded crystal, which leads to high GaN melting temperature, which is close to 2800 K [23]. It is well known that site atom

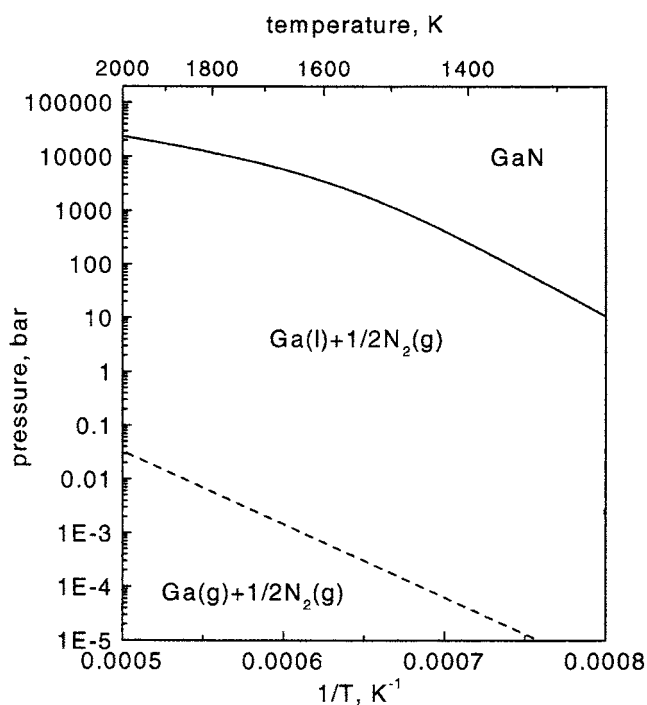


Figure 1. The triple-phase Ga(l)-N₂-GaN(s) equilibrium pressures: (a) Ga pressure, (b) N₂ pressure as a function of the inverse of the temperature.

diffusion processes attain observable rates for temperatures close to two-thirds of the melting temperature. For GaN, the estimated effective diffusion temperature is therefore about 1800 K. The corresponding equilibrium pressure is about 15 kbar. Therefore, for the site diffusion processes, the critical temperature range is between 1200 and 1500 °C. For other types of diffusion process these temperature should be lower.

In the experiments at such high temperatures, Ga evaporation can cause degradation or even evaporation of the GaN samples. Therefore for annealing GaN crystals or layers were covered by GaN powder. The evaporation of Ga from the powder increased the Ga partial pressure locally in the vicinity of the sample, preventing fast evaporation from the sample. The arrangement of the annealing experiment is schematically shown in figure 2(a).

The temperature is usually increased quite quickly, in most cases with the rate of 30 °C min⁻¹. Then for a prescribed time it was kept constant and lowered with the rate 50 °C min⁻¹ or quenched. The annealing times cited below refer to the duration of the application of constant annealing temperature. The typical time-temperature annealing profile is shown in figure 2(b).

3. Various diffusion regimes and different configurations of the experiments

The diffusion coefficients cannot be measured directly. The experimentally accessible observations include either the mean distance-time dependence, used in determination of tracer diffusion, or the change of the concentration profiles, used in determination of the chemical diffusion coefficient. In most cases we obtain the chemical diffusion coefficients, derived from the annealing time dependence of the concentration profiles.

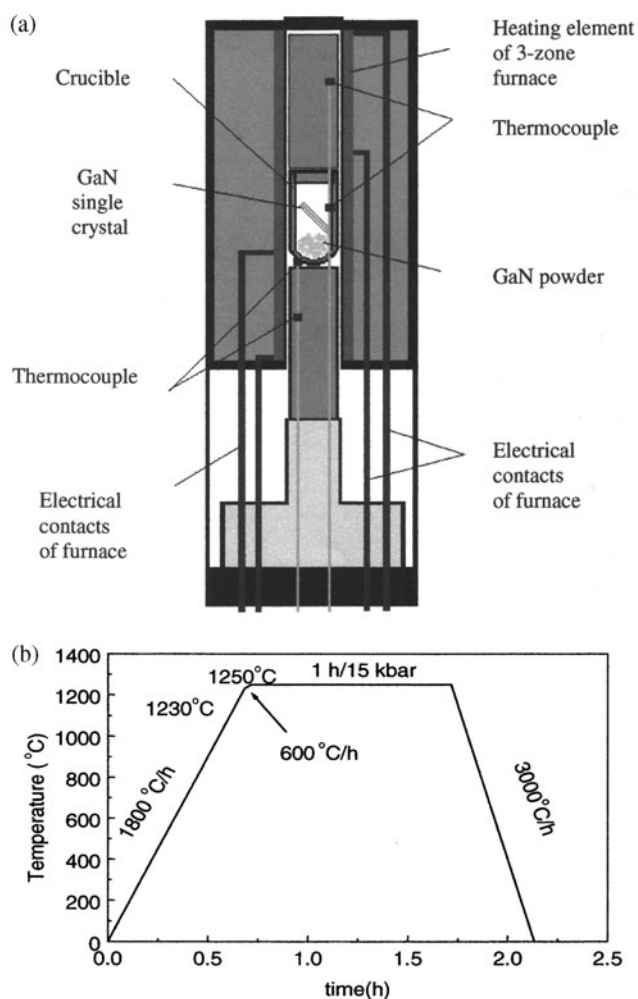


Figure 2. Experimental setup for annealing of nitride samples: (a) scheme of high pressure apparatus, (b) typical temperature–time annealing profile.

In our experiments three different configurations were used. In the first two cases, the foreign atoms diffuse from a localized external source, either limited in size or infinite. In virtually all cases one-dimensional geometry was chosen, with the source located on a flat surface of the nitride. Then the diffusion proceeds by one-dimensional spreading of the foreign atoms into the internal part of the sample. In the first case diffusion from metal atomic vapour sources was used. These metal vapours are characterized by relatively fast adsorption transition into the crystal of the vapour atoms. Since these processes are faster than diffusion into the solid interior, these sources keep the concentration of the foreign atoms constant at the edge of the sample. Then the distribution of the foreign atoms is given by the error function [19]

$$C = C_o \operatorname{erfc} \left[\frac{z}{2\sqrt{Dt}} \right] = C_o \left[1 - \frac{2}{\sqrt{\pi}} \int_0^{z/2\sqrt{Dt}} \exp(-x^2) dx \right] \quad (1)$$

where C_o is the concentration of the atoms at the edge and the z axis is perpendicular to the surface.

In the second case, the source of foreign species was a thin metal layer deposited on the surface of the sample. Then the diffusion proceeds with a limited amount of diffusing substance and is known as diffusion from an instantaneous source. The evolution in time leads to the change of the concentration at the edge of the sample. The short time evolution depends in a complicated manner on the thickness of the deposited layer and on the transition rate from the metal layer to the crystal. The asymptotic long time profile is universal and is given by the Gaussian function [19]

$$C = C_{\max}(t) \exp\left[-\frac{x^2}{4Dt}\right] = \frac{C_1}{\sqrt{\pi Dt}} \exp\left[-\frac{x^2}{4Dt}\right] \quad (2)$$

where $C_{\max}(t) \sim t^{-1/2}$ is the time dependent concentration at the edge of the sample. Since we will investigate the quenched spatial distribution of the metal concentration, the time dependence of this quantity will be not discussed here.

In the third case we have annealed the structure consisting of multiple QWs. The diffusion process is as before one dimensional but it involves multiple limited flat sources, located close to each other. These sources are characterized by an initial squarelike concentration distribution. In this case only rough estimates of the diffusion coefficients were possible, based on the time dependence of the average distance, characteristic to the tracer diffusion, which is given by the Einstein–Smoluchowski formula:

$$\lambda = 2\sqrt{Dt}. \quad (3)$$

By assuming that dissolution of the MQW structure occurs when the diffusion length λ , given by equation (3), is comparable with the distance between the wells, the estimate of the diffusion coefficient can be drawn.

One has to account for the fact that the diffusion coefficient, derived from the distribution given from equations (1) and (2), can be drastically changed by the presence of large density of the dislocations. To describe this influence, the Smoluchowski model will be used, in which the diffusion along the dislocation lines is approximated by the diffusion in the pipe of radius δ with the diffusion coefficient in the pipe given by D_d [19]. Assuming that $D_d \gg D$, the effective (measured) diffusion coefficient is given by

$$D_{eff} = D \left(1 + \frac{D_d \pi \delta^2 \rho}{D} \right) \quad (4)$$

where ρ is the dislocation density. In most cases it is assumed that the dislocation pipe radius δ is about 1–2 nm [19].

Using equations (3) and (4), three basic regimes can be distinguished, depending on the average diffusion distance and the dislocation density. The average distance between dislocations d , can be estimated using standard relation $d \approx \rho^{-1/2}$. As illustrated in figure 3, depending on the relation between λ and d , the three basic regimes can be distinguished:

- (i) $d \gg \lambda$, which is obeyed for low dislocation density. Then the second term in equation (4) can be neglected. The concentration profiles are described by equations (1) and (2) where the effective diffusion coefficient is equal to the volume diffusion coefficient D . This corresponds to the case of GaN single crystals and good quality homoepitaxial nitride layers where dislocation density is lower than 10^2 cm^{-2} .
- (ii) $d \sim \lambda$, which is obeyed for higher dislocation densities. Both terms in equation (4) are important and their ratio depends on the depth. Therefore the concentration profiles are not given by equations (1) and (2).
- (iii) $d \ll \lambda$, which is obeyed for high dislocation density. Then the second term in equation (4) is dominant and the first term can be neglected. The concentration profiles are described

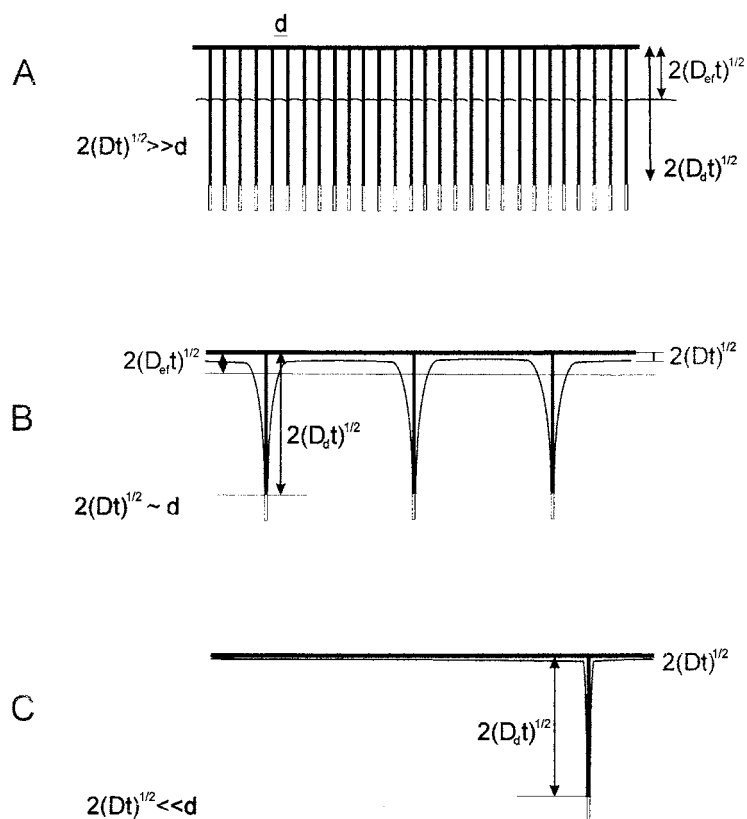


Figure 3. Three different regimes of the diffusion into the dislocated crystal: top—high, middle—average, bottom—low dislocation density.

by equations (1) and (2) where the effective diffusion coefficient is equal to the pipe diffusion coefficient D_d multiplied by the dislocation density dependent term. For GaN heteroepitaxial layers with a dislocation density of order of 10^{10} cm^{-2} and assuming that $\delta = 3 \text{ nm}$ this factor is equal to 3×10^{-3} .

4. Results of the annealing experiments. Diffusion coefficients

First the diffusion of Zn into a GaN single crystal and a GaN/ Al_2O_3 heteroepitaxial layer will be discussed. The dislocation density, estimated by the defect selective etching, was 10^2 cm^{-2} for the GaN single crystal and 10^9 cm^{-2} for the heteroepitaxial layer. The samples were annealed at $1350 \text{ }^\circ\text{C}$ for 500 min under nitrogen pressure of 10 kbar. The Zn concentration profile has been measured using the secondary ion mass spectrometer (SIMS) [15]. The SIMS results, presented in figure 4, show that the dislocation mediated diffusion is about four orders of magnitude faster than the bulk diffusion in the GaN crystal. Thus the above experiment indicates that the fundamental assumption of the Smoluchowski model that $D_d \gg D$ is fulfilled. From the shape of the diffusion profile it can be deduced that in the case of the bulk crystal the profile of Zn concentration is approximately described by equation (1). For the heteroepitaxial layer, however, the Zn concentration profile follows the exponential law,

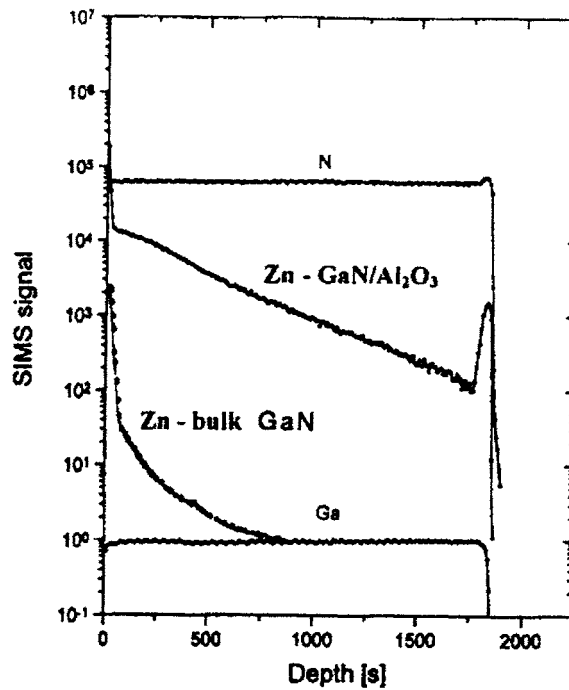


Figure 4. Zn concentration profiles obtained from SIMS measurements after annealing of GaN single crystals and heteroepitaxial layers.

which indicates that the duration of the annealing was such that the diffusion length λ was comparable with the average distance between dislocations d (middle or $d \sim \lambda$ case).

Diffusion of Zn and Mg into the GaN single crystal from the vapour source was investigated in more detail recently. The annealing experiment at the temperature 1200 °C under nitrogen pressure of 10 kbar lasted 240 min. The SIMS determined Zn and Mg concentration profiles are presented in figure 5(a). The obtained profiles were compared with the numerically inverted error function from equation (1), as shown in figure 5(b). As a result, the following diffusion coefficients were determined: for Mg $D_{\text{Mg}} = 1.6 \times 10^{-15} \text{ cm}^2 \text{ s}^{-1}$ and for Zn $D_{\text{Zn}} = 1.6 \times 10^{-14} \text{ cm}^2 \text{ s}^{-1}$. These data indicate that Mg diffuses much more slowly than Zn.

Diffusion of Au into GaN single crystals was investigated using deposited metal layer as a source. The samples were annealed under nitrogen pressure of 10 kbar for 120 min. Two different temperatures were used: 900 and 1400 °C. SIMS concentration profiles obtained from these experiments are shown in figure 6(a). These data were compared with the concentration dependence given by equation (2), as shown in figure 6(b). From this comparison the following diffusion coefficients of gold in GaN were obtained: for $T = 900 \text{ °C}$ $D_{\text{Au}} = 5.6 \times 10^{-15} \text{ cm}^2 \text{ s}^{-1}$ and for $T = 1400 \text{ °C}$ $D_{\text{Au}} = 1.3 \times 10^{-13} \text{ cm}^2 \text{ s}^{-1}$. From these values the energy barrier has been determined: $E_{\text{Au}}^{\text{bar}} = 1.1 \text{ eV}$.

Similar experiments were conducted with the diffusion of Au into the heteroepitaxial GaN/Al₂O₃ layers. The estimated dislocation density in these samples was about 10^{10} cm^{-2} . The samples were annealed under nitrogen pressure of 10 kbar for 10 min at three different temperatures: 900, 1050 and 1200 °C. The SIMS concentration profiles obtained from these experiments are shown in figure 7(a) while the comparison with the concentration dependence given by equation (2) is presented in figure 7(b). The following diffusion coefficients of

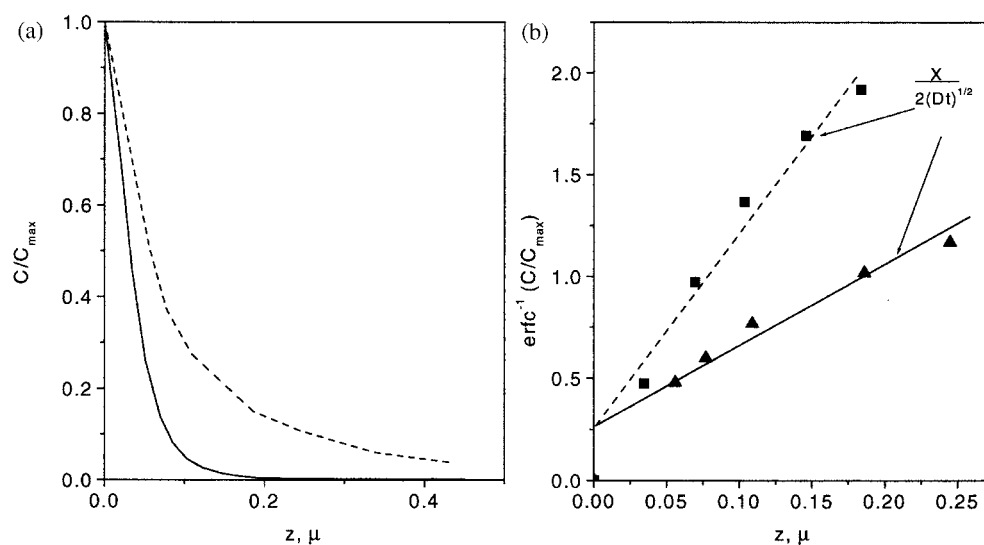


Figure 5. Zn and Mg concentration profiles obtained from SIMS measurements after annealing of GaN single crystals: (a) concentration profile, solid curve—Mg, dashed curve—Zn; (b) fit to the numerically obtained inverse of the error function of equation (1), triangles and solid line—Mg, squares and dashed line—Zn. Annealing parameters: $p_{N_2} = 10$ kbar, $T = 1200^\circ\text{C}$, $t = 240$ min.

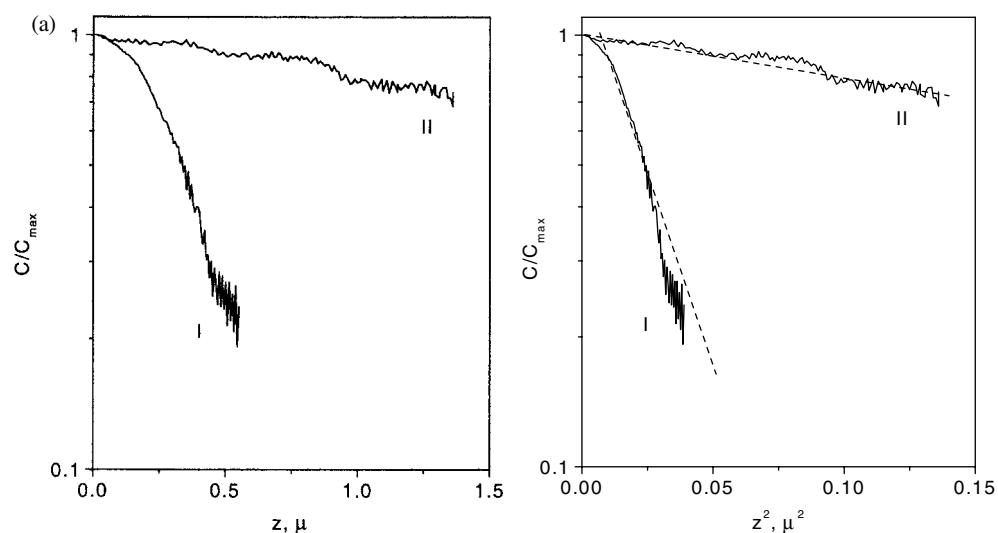


Figure 6. Au concentration profiles obtained from SIMS measurements after annealing of GaN single crystals: (a) concentration profile; (b) fit to error function from equation (2). Annealing parameters: $p_{N_2} = 10$ kbar, $t = 120$ min, line I— $T = 900^\circ\text{C}$, line II— $T = 1400^\circ\text{C}$.

gold in GaN/Al₂O₃ were obtained: for $T = 900^\circ\text{C}$ $D_{\text{Au}} = 1.7 \times 10^{-13} \text{ cm}^2 \text{ s}^{-1}$, for $T = 1050^\circ\text{C}$ $D_{\text{Au}} = 2.3 \times 10^{-12} \text{ cm}^2 \text{ s}^{-1}$ and for $T = 1200^\circ\text{C}$ $D_{\text{Au}} = 4.1 \times 10^{-12} \text{ cm}^2 \text{ s}^{-1}$. Assuming that the concentration dependent factor in equation (4) was 3×10^{-3} , the pipe diffusion coefficients were $D_d = 5.1 \times 10^{-10} \text{ cm}^2 \text{ s}^{-1}$, $D_d = 6.9 \times 10^{-9} \text{ cm}^2 \text{ s}^{-1}$ and

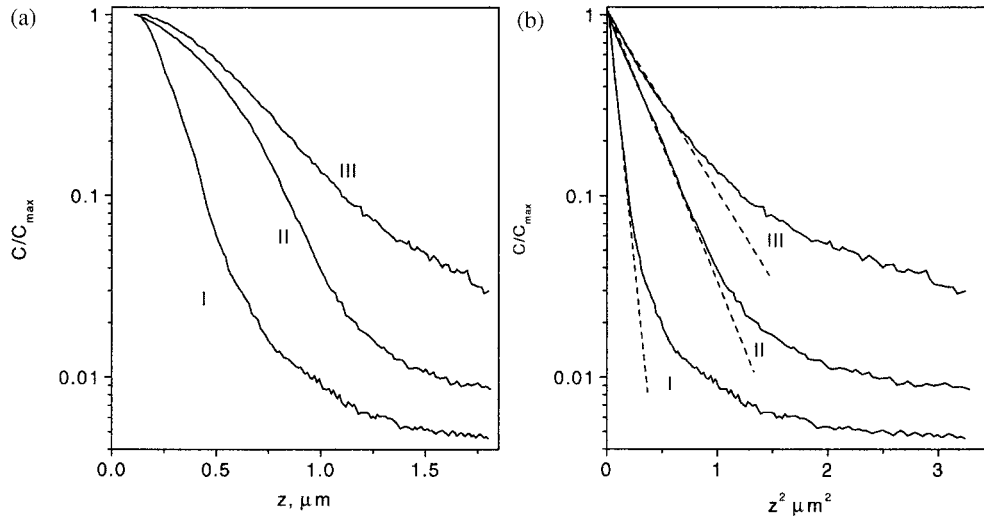


Figure 7. Au concentration profiles obtained from SIMS measurements after annealing of heteroepitaxial GaN/Al₂O₃ layers: (a) concentration profile; (b) fit to error function from equation (2). Annealing parameters: $p_{N_2} = 10$ kbar, $t = 10$ min. Line I— $T = 900$ °C, line II— $T = 1050$ °C, line III— $T = 1200$ °C.

$D_d = 1.2 \times 10^{-8}$ cm² s⁻¹ for these three temperatures respectively. From the temperature dependence the energy barrier has been determined: $E_{Au}^{bar} = 0.62$ eV. So a large difference between the energy barriers for single crystals and heteroepitaxial layers indicates that bulk diffusion and dislocation mediated diffusion proceed via different microstates.

During implantation, the crystalline structure of the sample is destroyed, especially in the vicinity of the implanted atoms. The lattice has to be rebuilt and additionally the implanted impurities have to move into the lattice positions to become electrically and optically active. The Zn and Mg implanted layers were annealed under high N₂ pressure at various temperatures. The annealing time was 15 min for Mg and 60 min for Zn implanted samples. The photoluminescence (PL) spectrum of the Mg implanted layer, presented in figure 8, shows that the activation of the sample at temperature lower than 1200 °C is negligible. For temperatures between 1300 and 1500 °C, the optical activity of the sample increases with the annealing temperature. Using higher temperatures does not bring any further increase of the PL of the sample. For the Zn implanted sample the PL dependence on the annealing temperature is shown in figure 9. The increase of optical activity of the Zn implanted samples occurs for the annealing temperatures between 1150 and 1450 °C. These results show that in this temperature range the mobility of native Ga and N atoms and also the implanted Mg and Ga atoms attains measurable rates.

These conclusions were confirmed by the annealing experiments with the MQWs AlGaN/GaN and InGaN/GaN structures. As shown in figure 10 for the GaN/InGaN/GaN MQW structure grown on sapphire substrate, the annealing for 30 min at $T = 1300$ °C does not and at $T = 1400$ °C does lead to the dissolution of the structure. Assuming that the diffusion length is equal to half of the width of the well, i.e. $\lambda = 2.5$ nm, the following estimate of the diffusion coefficient of In in GaN can be obtained: $D_{In} \sim 5 \times 10^{-18}$ cm² s⁻¹. Similar experiments were conducted using near dislocation-free homoepitaxial AlGaN/GaN/AlGaN MQWs grown on GaN substrates. The wells were investigated by x-ray diffraction. The results of these investigations, presented in figure 11, show that the structure is stable at 1400 °C and

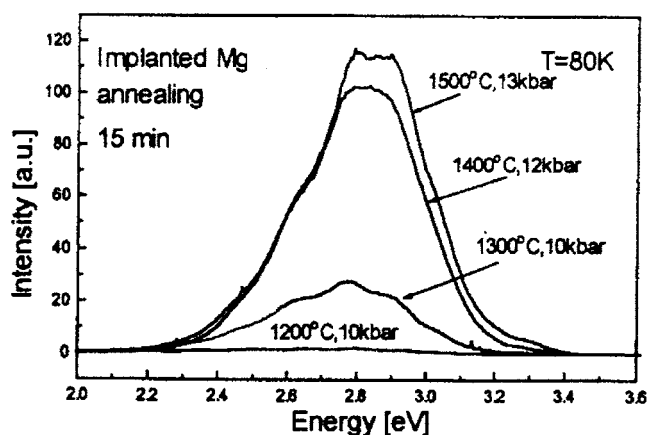


Figure 8. PL spectra of Mg implanted GaN layers. Annealing time $t = 15$ min.

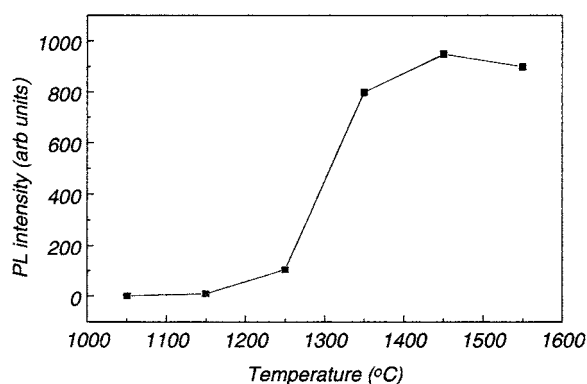


Figure 9. Temperature dependence of PL intensity of Zn implanted GaN layers. Annealing parameters: $p_{N_2} = 16$ kbar, $t = 60$ min.

unstable at 1500°C . From these data the diffusion coefficient of Al in GaN at 1500°C was estimated: $D_{\text{Al}} = 1.3 \times 10^{-17} \text{ cm}^2 \text{ s}^{-1}$.

The comparison of these results shows that the dissolution of MQW structures does not depend in significant degree on the density of dislocations. This is different from the above reported results concerning the diffusion from external sources. The diffusion from the external sources proceeds quickly along the dislocation lines and then spreads laterally. In the case of dissolution of MQW structures, the impurities have to reach the dislocation lines first, which is a slow rate controlling process. Therefore fast diffusion along dislocation lines does not affect the dissolution process. This explains why the MQW structures are stable in highly dislocated heteroepitaxial layers. The same process controls the stability of p-n junctions in LEDs and LDs.

The group III metal diffusion coefficients can be compared with the temperature dependence of the diffusion coefficients obtained for other III-V compounds. The comparison has been made in figure 12. As presented, the estimated diffusion coefficients are in good agreement with the data obtained for arsenides, phosphides and antimonides [20]. The data for GaN, obtained using GaN/Al₂O₃ samples by Ambacher *et al*, are eight orders of magnitude

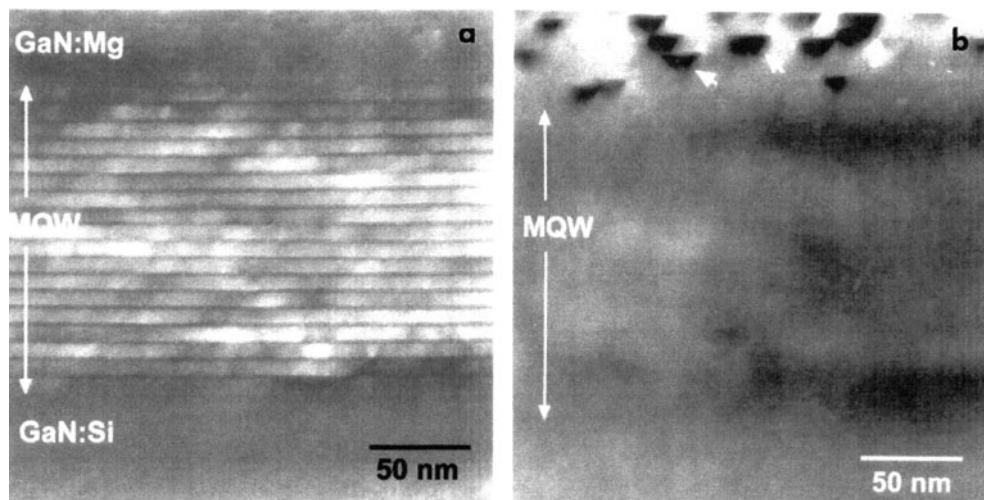


Figure 10. TEM of GaN/In_{0.1}Ga_{0.9}N/GaN MQW structure grown on sapphire [22]. Annealing parameters: $p_{N_2} = 16$ kbar, $t = 60$ min. Upper part— $T = 1300$ °C, lower part— $T = 1400$ °C.

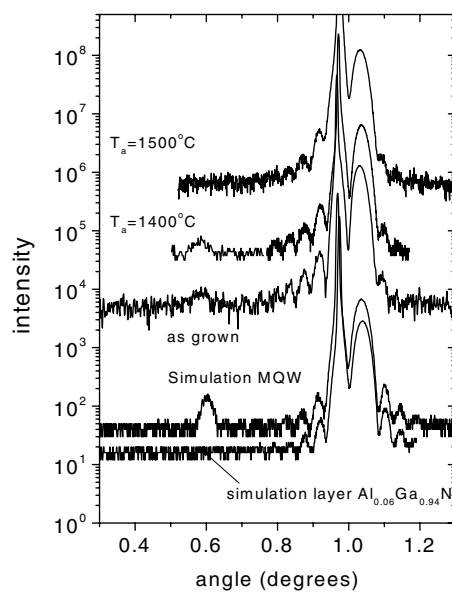


Figure 11. X-ray diffraction pattern of annealed Al_{0.06}Ga_{0.84}N/GaN/Al_{0.06}Ga_{0.84}N MQW structure. Annealing parameters: $p_{N_2} = 16$ kbar, $t = 2000$ s. For comparison, the simulation MQW structure and a single layer are demonstrated.

higher [21]. Most likely they were obtained at too low temperatures where the mobility of the atoms is negligible. Therefore the resulting concentration changes were too small to be detected by the SIMS technique used by Ambacher *et al* [21].

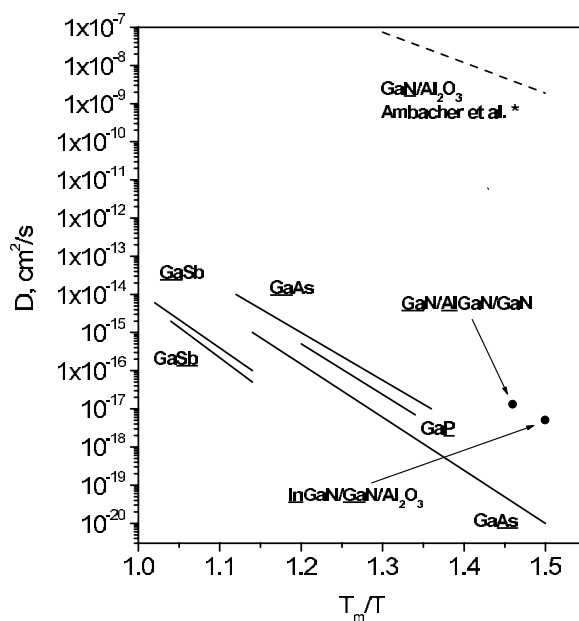


Figure 12. Temperature dependence of selfdiffusion coefficients for different III–V compounds. Solid lines—[20]; dashed lines—[21], points—this work. The chemical symbol of the diffusion element is underlined.

5. Summary

The results reported in this paper can be summarized as follows.

- (a) Diffusion in GaN is still not a well investigated phenomenon because of
 1. low purity of the nitride materials $N_d > 10^{17} \text{ cm}^{-3}$
 2. low structural quality of the layers obtained by low pressure MOCVD and MBE methods on foreign substrates
 3. high thermal stability of quantum structures (QWs, p–n junctions)—selfdiffusion begins at 1800 K, which requires 15 kbar of N_2 pressure.
- (b) High diffusion coefficients, measured for impurities Au, Zn and Mg in heteroepitaxial layers, are related to fast diffusion along the dislocation lines.
- (c) Selfdiffusion in GaN follows the dependence observed in other Ga–V compounds.
- (d) For low pressure MOCVD and MBE the nitride growth conditions bulk selfdiffusion is negligible.
- (e) Due to very low bulk diffusion coefficient D , the p–n junctions and the QWs are very stable for both low dislocation density (10^2 dislocations cm^{-2}) and high dislocation density (10^{10} dislocations cm^{-2}) structures.

Acknowledgment

The research presented in this paper has been supported by Poland's Committee for Scientific Research grants 2700/C. T11-8/2000 and 2 P03B 025 17.

References

- [1] Amano H, Kito M, Hiramatsu K and Akasaki I 1989 *Japan. J. Appl. Phys. 2, Lett.* **28** L2112
- [2] Nakamura S, Mukai T, Senoh M and Iwasa N 1992 *Japan. J. Appl. Phys. 2, Lett.* **31** L139
- [3] Nakamura S, Senoh M and Mukai T 1993 *Japan. J. Appl. Phys. 2, Lett.* **32** L8
- [4] Nakamura S, Senoh M, Iwasa N and Nagahama S 1995 *Japan. J. Appl. Phys. 2, Lett.* **34** L797
- [5] Nakamura S, Senoh M, Nagahama S, Iwasa N, Yamada T, Matsushita T, Kiyoku H and Sugimoto Y 1996 *Japan. J. Appl. Phys. 2, Lett.* **35** L74
- [6] Nakamura S 2000 *Mater. Sci. Forum* pt 2 **338–342** 1609
- [7] Liliental-Weber Z and Cherns D 2001 *J. Appl. Phys.* **89** 7833
- [8] Grzegory I 2002 *J. Phys.: Condens. Matter* **14**
- [9] Kirchner C, Schwegler V, Eberhard F, Kamp M, Ebeling K J, Prystawko P, Leszczynski M, Grzegory I and Porowski S 2000 *Prog. Cryst. Growth Character. Mater.* **41** 57
- [10] Okamoto Y, Saito M and Oshiyama A 1996 *Japan. J. Appl. Phys. 2, Lett.* **35** L807
- [11] Suski T, Litwin-Staszewska E, Perlin P, Wisniewski P, Teisseyre H, Grzegory I, Bockowski M, Porowski S, Saarinen K and Nissila J 2002 *J. Cryst. Growth* **230** 368
- [12] Litwin-Staszewska E, Suski T, Piotrkowski R, Grzegory I, Bockowski M, Robert J L, Konczewicz S, Wasik D, Kaminska M, Cote D and Clerjaud B 2001 *J. Appl. Phys.* **89** 7960
- [13] Suski T, Perlin P, Leszczynski M, Teisseyre H, Grzegory I, Jun J, Bockowski M, Porowski S, Pakula K, Wyszomolek A and Baranowski J M 1996 Gallium nitride and related materials *1st Int. Symp. Mater. Res. Soc.* (Pittsburgh, PA: Materials Research Society) pp 15–25
- [14] Ohuchi Y, Tadamoto K, Nakayama H, Kaneda N, Detchprohm T, Hiramatsu K and Sawaki N 1997 *J. Cryst. Growth* **170** 325
- [15] Porowski S, Jun J, Krukowski S, Grzegory I, Leszczynski M, Suski T, Teisseyre H, Foxon C T and Korakakis D 1999 *Physica B* **265** 295
- [16] Barun I 1994 *Thermochemical Data of Pure Substances* 3rd edn (Weinheim: VCH)
- [17] Karpinski J, Jun J and Porowski S 1985 *J. Cryst. Growth* **66** 1
- [18] Van Vechten J A 1973 *Phys. Rev. B* **7** 1479
- [19] Kaur I and Gust W 1988 *Fundamentals of Grain and Interphase Boundary Diffusion* (Stuttgart: Ziegler)
- [20] Stolwijk N A, Bosker G and Popping J 2001 *Defect Diffusion Forum* **194–199** 687
- [21] Ambacher O, Freudberg F, Dimitrov R, Angerer H and Stutzman M 1998 *Japan. J. Appl. Phys.* **37** 2416
- [22] Romano T L, McCluskey M D, Vande Walle C G, Northrup J E, Bour D P, Kneissi M, Suski T and Jun J 1999 *Appl. Phys. Lett.* **75** 3950